Journal of Sustainability for Energy
https://www.acadlore.com/journals/JSE

Experimental Exergy Analysis of Air Flow Through Micro Helical Tubes with Novel Geometries under Adiabatic Conditions

Razieh Abbasgholi Rezaei*

Department of Mechanical Engineering, Urmia University, 5756151818 Urmia, Iran

* Correspondence: Razieh Abbasgholi Rezaei (r_rezaei_mec@yahoo.com)

Received: 02-05-2023 **Revised:** 03-13-2023 **Accepted:** 03-20-2023

Citation: R. A. Rezaei, "Experimental exergy analysis of air flow through micro helical tubes with novel geometries under adiabatic conditions," *J. Sustain. Energy*, vol. 2, no. 1, pp. 29–38, 2023. https://doi.org/10.56578/jse020103.

Abstract: Helical microtubes are commonly used in micro-electronic cooling techniques and micro-heat exchangers because of the creation of secondary flows, which leads to greater temperature and velocity gradients. It is of great significance to further improve the overall efficiency of the helical microtubes so as to diminish energy consumption. This experimental work mainly focuses on exergy analysis of air flow through adiabatic helical microtubes with circle, triangle, square, and pentagon geometries with circular cross section. The temperature rises due to viscose dispassion and pressure drops have been measured for all adiabatic helical coils in the laminar flow range. To identify irreversibility of flow, rate of air flow, coil diameter and Dean number are varied to investigate their influences on the entropy generation. Also, the second law of thermodynamics was applied to recognize exergy efficiencies and to determine true magnitudes of exergy losses. Results indicate that entropy generation increases by increasing the flow rate and the coil diameters in all geometries, however, the exergy efficiency decreases. By considering geometry, in constant flow rate and identical coil diameter, the highest entropy generation can be approximately observed in the triangles, squares, pentagons, and circles, respectively. Moreover, the proportions of theoretical exergy losses to actual exergy losses have been computed for all geometries in order to probe the viscous heating effects and it is found that the predicted exergy losses distinguish substantially from measured amounts due to viscose dispassion.

Keywords: Second law analysis; Entropy generation; Helical microtube; Viscose dispassion; Exergy efficiency

1 Introduction

In recent years, helical microtubes have had a significant role in improving thermal performance in industrial applications, such as micro shell and tube heat exchangers due to the excellent processing and anti-fouling performance. Owing to the extensive use of these heat exchange equipment, any slight performance improvement of them will yield substantial economic benefits. Theses microtubes generate greater temperature and velocity gradients compared to macro tubes by the creation of secondary flows [1–3]. Since any change in the flow gives rise to the larger impact, second law analysis of thermodynamic is indispensable. The exergy loss is a measure to evaluate the thermodynamic efficiency of the process, in the other words, the lower exergy loss means the higher thermodynamic efficiency and the lower required energy, which can be achieved by debilitating irreversibility through friction, mixing, chemical reactions, heat transfer, and etc. In the present study, exergy losses are investigated in helical microtubes with novel geometries under adiabatic conditions to discover the effects of viscous dissipation.

The concept of irreversibility in a straight pipe with a circular cross-section firstly was surveyed by Bejan [4]. Ozalp [5] computationally detected the effects of temperature difference, Prandtl number and Eckert number on exergy loss and entropy generation in a micropipe, and he discovered that for Poiseuille flow the local exergy loss greatly differs from the entropy generation due to the presence of pressure drop. He also solved the Navier-Stokes and energy equations for various Reynolds numbers and surface roughness at constant heat fluxes and discussed heat transfer-frictional characteristics on entropy generation [6]. Dizaji et al. [7] performed a comprehensive study of experimental exergy analysis for tube-in-tube helically coiled heat exchangers. Results indicated that the enhancement of hot or cold-water flow rates, hot water inlet temperature, and coil diameter increase the amount of exergy loss. Pourhedayat et al. [8] proposed a new empirical correlation to predict the dimensionless exergy loss in helical tubes. Moradi et al. [9] studied thermal and entropic characteristics of upward air-water two-phase flow in a vertical helical tube. Their results indicate maximum increment of 35% and 26% for heat transfer coefficient and entropy

generation, respectively. Ko and Ting [10] presented the thermodynamic optimization of fully developed laminar convection in a helical coil. The optimal helical coil design from the perspective of the thermodynamic second law was introduced in their investigation. Parlak et al. [11] probed the Second law analysis of water flow through smooth microtubes under adiabatic conditions and their results disclosed that the flow characteristics in the smooth microtubes distinguish substantially from the conventional theory for flow in the larger tubes with respect to viscous heating dissipation. They also conducted exergy analysis of laminar fluid flow in stainless steel microtubes and it was observed that as Re increases, measured exergy losses were significantly higher than that of the predicted values [12]. In summarizing the above literature review, the number of studies related to micro helical tubes is so limited. On the other hand, curved geometries of triangle, square, and pentagon with circular cross section have not been examined. Accordingly, this motivates this investigation to assess the rate of entropy generation, exergy loss, and exergy efficiency of helical microtubes with circle, triangle, square, and pentagon geometries with circular cross section under adiabatic conditions to fill the gap between friction factor and the geometrical optimization study of the helical microtubes based on the second law of thermodynamics and provides strong evidence that the exergy destruction minimization principle is applicable in the laminar flow regime of helical microtubes. In this study, the effects of flow rate, coil diameter and Dean number on entropy generation were investigated. It should be hinted that on account of conducting experiments under adiabatic conditions, the effect of heat transfer was disregarded.

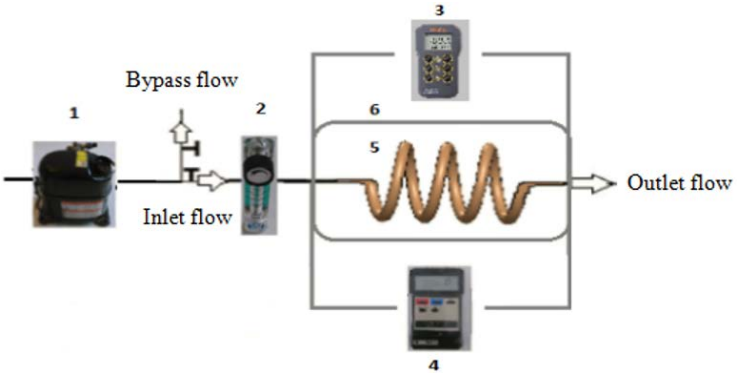

Figure 1. The schematic illustration of the test set-up: 1- Compressor, 2- Air rota-meter, 3- Thermocouple, 4- Manometer, 5- Microtubes, and 6- Isolated test part

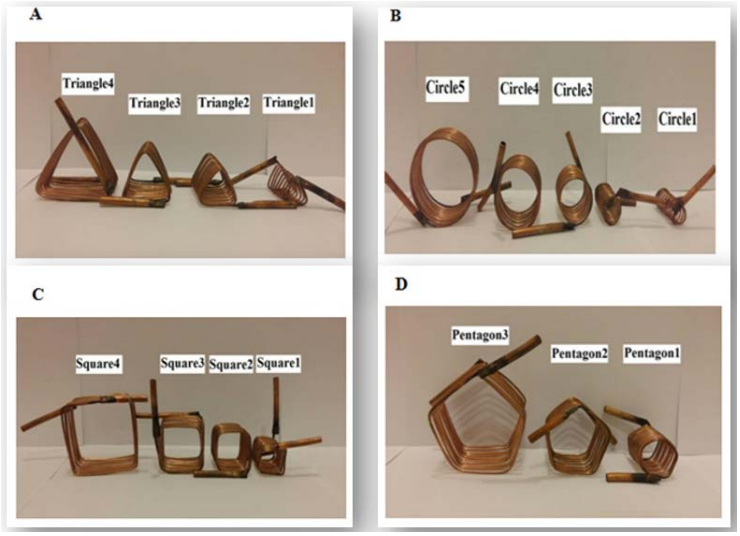

Figure 2. Various investigated geometries with different coil diameter: (A) Circle, (B) Triangle, (C) Square, and (D) Pentagon [13]

A general view of the experimental set-up is depicted in Figure 1. As seen, the supplied air flow by a compressor at 20°C in five distinct flow rates which were determined as 1, 1.5, 2, 2.5, and 3 l/min was entered to a helical microtube. Two valves were used to control the air flow rate, first one was assembled at the main path and the second one was provided to control the bypass flow. It is remarkable that the air flow rate produced by air compressor was more than the maximum measurable rate of air-Rota-meter; so that the bypass flow was provided to a precise control

of air flow rate. The measurement of air flow rate, temperature, and the pressure drop at both the entrance and the exit cross-section of the microtubes were carried out by air-Rota-meter, K-type thermocouple (accuracy $\pm 0.5^{\circ}\mathrm{C}$ and resolution $0.1^{\circ}\mathrm{C}$), and digital manometer (accuracy and resolution 1 mmHg), respectively. Four distinguishing geometries, such as circle, triangle, square, and pentagon with various coil diameters were located in the adiabatic test section, which was isolated by applying glass wool. To minimize the heat loss to the environment, an air gap of 2-3 mm was considered between the test tube and the isolating material. Furthermore, in a particular temperature-controlled test room, where temperature fluctuation was periodically checked by means of a portable temperature measurement device, the least heat loss from the tube surface to the surrounding air was achieved by minimizing temperature differences between the tube surface and the surrounding air to $0.5^{\circ}\mathrm{C}$. The inspected microtubes are demonstrated in Figure 2.

2 Experimental Uncertainty

To compute the uncertainty in this study, the method proposed by Moffat [14] was exploited. The following equation represents the uncertainty when a result (W_R^+) is to be calculated:

$$W_R^+ = \left[\left(\mathrm{W}_1 \frac{\partial R^+}{\partial X_1}\right)^2 + \left(\mathrm{W}_2 \frac{\partial R^+}{\partial X_2}\right)^2 + \cdots + \left(\mathrm{W}_\mathrm{n} \frac{\partial R^+}{\partial X_n}\right)^2\right]^{0.5} \tag{1}$$

where, $W_\mathrm{i}(i = 1, 2, \ldots, \mathrm{n})$ expresses the uncertainty values associated with the independent variable $(X_\mathrm{i}(i = 1, 2, \ldots, \mathrm{n}))$.

For example, entropy generation rates uncertainties can be calculated as shown below:

Substituting Eq. (15) into Eq. (1) yields;

$$\begin{aligned} W_{s^\circ_{gen}}^+ &= \left[\left(\frac{\partial {s^\circ_{gen}}^+}{V^\circ}\ W_{V^\circ}\right)^2 + \left(\frac{\partial {s^\circ_{gen}}^+}{\partial \Delta P} W_{\Delta P}\right)^2 + \left(\frac{\partial {s^\circ_{gen}}^+}{\partial T_{in}} W_{T_{in}}\right)^2\right]^{0.5} \\ &= \left[\left(\frac{\Delta P}{T_{in}} W_{V^\circ}\right)^2 + \left(\frac{V^\circ}{T_{in}} W_{\Delta P}\right)^2 + \left(-\frac{\Delta P}{T_{in}^2} W_{T_{in}}\right)^2\right]^{0.5} \end{aligned} \tag{2}$$

By multiplying $\left(1/s^\circ_{gen}\right)$ in two side of Eq. (2);

$$\frac{W_{s^\circ_{gen}}^+}{s^\circ_{gen}} = \left[\left(\frac{W_{V^\circ}}{V^\circ}\right)^2 + \left(\frac{W_{\Delta P}}{\Delta P}\right)^2 + \left(-\frac{W_{T_{in}}}{V^\circ T_{in}}\right)^2\right]^{0.5} \tag{3}$$

The uncertainties calculated in this study are summarized in Table 1.

Table 1. Uncertainty values of different parameters

Parameter	Comment
Pressure drop	2.6%
Reynolds number	2.7%
Inlet temperature	0.6%
Dean number	2.8%
Total entropy generation of circle	3.3%
Total entropy generation of square	3.7%
Total entropy generation of triangle	3.8%
Total entropy generation of pentagon	3.4%
Exergy efficiency of circle	3.4%
Exergy efficiency of square	3.8%
Exergy efficiency of triangle	3.9%
Exergy efficiency of pentagon	3.5%
Confidence interval	95%

3 Exergy Analysis

The results section may be divided into subsections. It should describe the results concisely and precisely, provide their interpretation, and draw possible conclusions from the results.

3.1 Exergy Loss

The rate of exergy change in a control volume is equal to the rate of exergy transfer through the control volume boundary by heat, work, and mass flow minus the rate of exergy destruction.

$$\begin{aligned}\frac{dX_{cv}}{dt} &= -W^{\circ} - X^{\circ}_{\text{loss}} + \sum\left(1-\frac{T_0}{T_s}\right)Q^{\circ} + \sum_{\text{in}} m^{\circ}\psi - \sum_{\text{out}} m^{\circ}\psi \\ &= -W^{\circ} - X^{\circ}_{\text{loss}} + \sum\left(1-\frac{T_0}{T_s}\right)Q^{\circ} + \sum m^{\circ}\left((h_{\text{in}} - h_{\text{out}}) - T_0\left(s_{\text{in}} - s_{\text{out}}\right)\right)\end{aligned} \tag{4}$$

Exergy loss in a control volume for a steady state flow under adiabatic conditions can be expressed as;

$$X^{\circ}_{\text{loss}} = m^{\circ}\left(h_{\text{in}} - h_{\text{out}}\right) - m^{\circ}T_0\left(s_{\text{in}} - s_{\text{out}}\right) \tag{5}$$

From the first law of thermodynamics;

$$\frac{dE_{cv}}{dt} = W^{\circ} - Q^{\circ} + \sum_{in} m^{\circ}h - \sum_{\text{out}} m^{\circ}h \tag{6}$$

$$0 = h_{in} - h_{out} \tag{7}$$

And the exergy loss equation simplifies into:

$$X^{\circ}_{\text{loss}} = m^{\circ}T_0\left(s_{\text{out}} - s_{\text{in}}\right) \tag{8}$$

Two possible irreversibility mechanisms for any fluid flow responsible for exergy losses are heat transfer and pressure drop through the passage. So, the rate of entropy generation can be considered that;

$$S^{\circ}_{gen} = S^{\circ}_{gen,\Delta T} + S^{\circ}_{gen,\Delta p} \tag{9}$$

However, the irreversibility in the effect of heat transfer is negligible under adiabatic conditions.

The second law of thermodynamics can be expressed for steady state flow through the pipe segment as a control volume (Figure 3) as following;

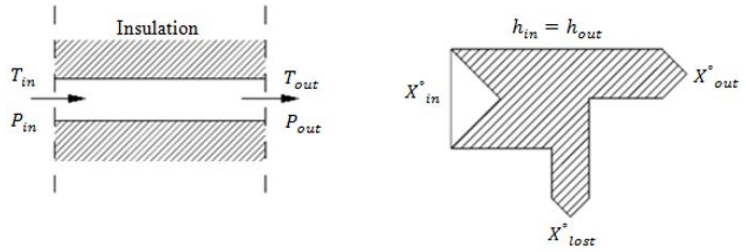

Figure 3. Control volume and corresponding irreversibility owing to fluid friction

$$\frac{dS_{cv}}{dt} = S^{\circ}_{gen} + \sum\frac{Q^{\circ}}{T} + \sum_{in} m^{\circ}s - \sum_{\text{out}} m^{\circ}s \tag{10}$$

Can simplifies into;

$$S^{\circ}_{\text{gen}} = \dot{m}\left(s_{\text{out}} - s_{\text{in}}\right) \tag{11}$$

In addition, the Gibbs equation represents that;

$$Tds = dh - vdp \tag{12}$$

By integrating Eq. (12) from inlet to the outlet and exerting the first law (dh=0), it can be obtained;

$$\int_{in}^{\text{out}} ds = -\int_{in}^{\text{out}} \frac{vdp}{T} = -\int_{in}^{\text{out}} R\frac{dp}{p} \tag{13}$$

By substituting Eq. (13) into Eq. (11), the S°_{gen} is expressed as;

$$S^{\circ}_{gen} = \int_{in}^{out} \dot{m} ds = -\int_{in}^{out} \dot{m} R \frac{dp}{p} = \dot{m} R \frac{\Delta p}{p} = \dot{m} \frac{\Delta p}{\rho T_{in}} = \frac{\dot{V} \Delta p}{T_{in}} \tag{14}$$

Finally, the exergy loss on account of the entropy generation is obtained as follows;

$$X^{\circ}_{\text{loss}} = m^{\circ} T_0 \left(S_{\text{out}} - S_{\text{in}} \right) = T_0 S^{\circ}_{\text{gen}} = \dot{V} \Delta p \tag{15}$$

Hence, the decrease in exergy is proportional to the pressure drop as well as the mass flow rate.

Also, to predict exergy loss caused by friction Eq. (17) is developed by substituting the pressure drop caused by friction, Eq. (16) [13], into Eq. (15);

$$\Delta P = f_c \rho l V^2 / 2 d_{inn} \tag{16}$$

$$\left(X^{\circ}_{loss}\right)_{predicted} = \left[\frac{f_c \rho l V^2}{2 d_{in}} * \dot{V} \right] \tag{17}$$

where V, d_{in}, l, ρ, and f_c are inlet velocity, coil inner diameter, tube length before coiling operation, density and empirical correlations for the friction factor of assumed helical microtubes in laminar flow regime presented in Table 2.

Table 2. Empirical correlation of friction factors for helical microtubes [13]

Geometry	Friction Factor
Circle	$f_c = 97.499 Re^{-0.808} \left(\frac{d_{inn}}{D_c}\right)^{-0.549}$
Triangle	$f_c = 98.175 Re^{-0.798} \left(\frac{d_{inn}}{D_c}\right)^{-0.455}$
Square	$f_c = 59.841 Re^{-0.818} \left(\frac{d_{inn}}{D_c}\right)^{-0.668}$
Pentagon	$f_c = 117.490 Re^{-0.903} \left(\frac{d_{inn}}{D_c}\right)^{-0.691}$

3.2 Exergy Efficiency

Exergy efficiency illustrates the how far the efficiency of a conversion process is from its theoretical maximum. The universal exergy efficiency enables a thermodynamic comparison of alternative systems in cases where no product can be defined. Universal exergy efficiency is defined as [15];

$$\eta_{\text{ex},u} = \frac{\sum X_{\text{out}}}{\sum X_{\text{in}}} = \frac{\sum X_{\text{in}} - X_{\text{loss}}}{\sum X_{\text{in}}} = 1 - \frac{\sum X_{\text{loss}}}{\sum X_{\text{in}}} \tag{18}$$

The exergy transfer to a steady-flow system is equal to the exergy transfer from it plus the exergy loss within the system.

$$X^{\circ}_{\text{in}} = X^{\circ}_{\text{out}} - X^{\circ}_{\text{loss}} \tag{19}$$

Thus, in this case,

$$\eta_{\text{ex},u} = 1 - \frac{T_0 \left(s_{\text{out}} - s_{\text{in}} \right)}{\left(h_{\text{in}} - h_0 \right) - T_0 \left(s_{\text{in}} - s_0 \right)} = 1 - \frac{\Delta P}{\rho R T_0 \ln \frac{P_{\text{in}}}{P_0}} \tag{20}$$

In Eq. (20), *R* is the specific ideal gas constant of the air, which is equal to 0.287 $\left[KJ(KgK)^{-1}\right]$.

4 Discussion

An exergy analysis was performed for air flow through the aforementioned geometries. The entropy generation rate in the flow was calculated by Eq. (14). According to Figure 4, entropy generation rate increases as flow rate and coil diameter increase in each geometry. It is obvious that the tube length not only intensifies pressure drop, it can be deduced from Eq. (16), but also affects the exergy loss as expected, without revealing any unusual behavior as Parlak et al. [12] revealed.

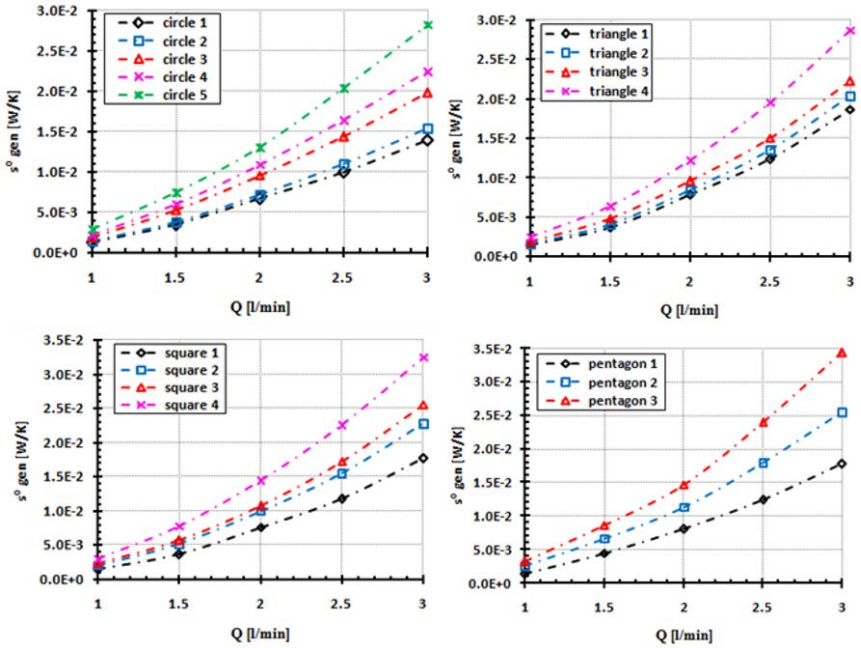

Figure 4. Rate of entropy generation versus flow rate in different coil diameters of A) Circles, B) Triangles, C) Squares, D) Pentagons

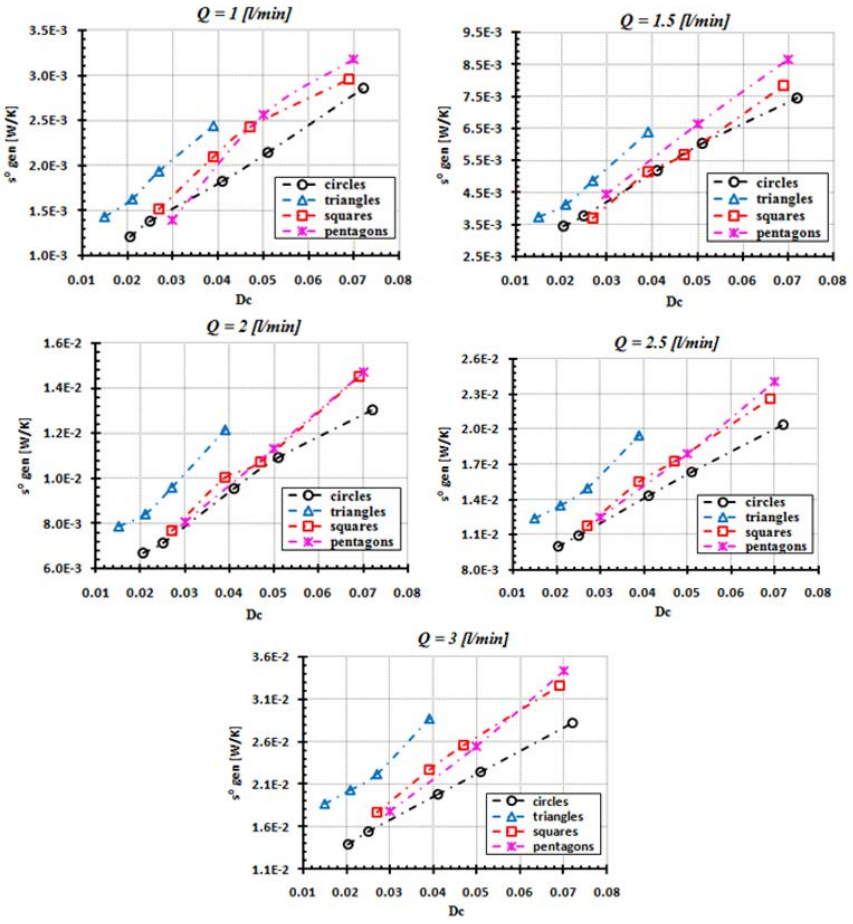

Figure 5. Rate of entropy generation versus coil diameter for all geometries at constant flow rates

For better understanding of the impact of coil diameters, entropy generation rate versus coil diameter at constant flow rates (1, 1.5, 2, 2.5, and 3 l/min) is illustrated in Figure 5 that demonstrates greater entropy generation occurs in

triangle, square, pentagon and circle, respectively because of greater minor losses of pressure caused by bend angle in geometries.

The dimensionless Dean number in helical tubes plays the role of Reynolds number in the straight pipes. It gives the ratio of the viscous force acting on a fluid flowing in a curved pipe to the centrifugal force. The Dean number is defined as,

$$D_e = Re\,(d_{inn}/D_c)^{0.5} \tag{21}$$

As disclosed in Figure 6 at constant flow rates, higher entropy generations occur both in larger coil diameters and in lower Dean numbers. In the analysis based on geometry, in constant flow rate and assuming identical Dean number, almost the highest entropy generations take place in triangles, squares, pentagons, and circles respectively. The numbers on the diagram indicate the orientation of expanding coil diameters for each of geometries where 1 represents the smallest diameter.

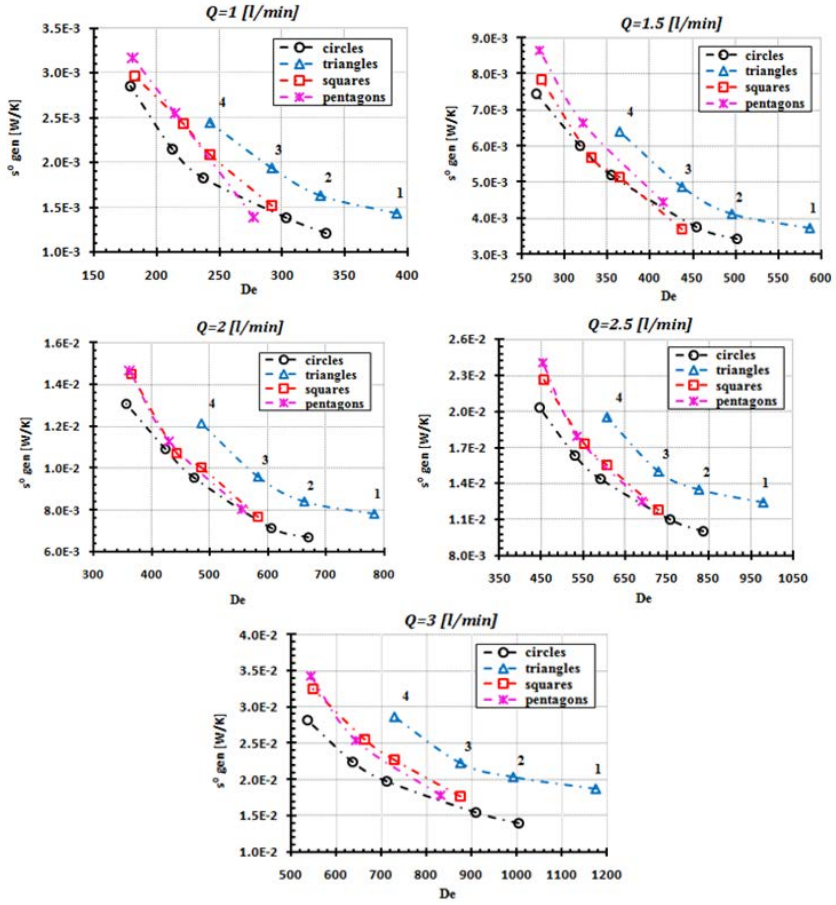

Figure 6. Rate of entropy generations versus Dean number in different coil diameters at constant flow rates for all geometries

In Figure 7, the proportions of theoretical exergy losses to actual exergy losses have been computed for all geometries in order to probe the viscous heating effects. The actual exergy losses are calculated by Eq. (15), by multiplying the measured pressure loss with volumetric flow rate under experimental conditions. And theoretical exergy losses caused by friction are predicted by Eq. (17), where ρ and f (function of Reynolds number) are thermophysical properties and varying with temperature. These thermophysical properties are theoretically calculated at the inlet temperature and assumed to be constant which means viscous heating effect was not taken into account. The Figure 7 reveals that the viscous heating effects have noticeable impact in exergy losses in all geometries.

The major aim of exergy analysis is to recognize exergy efficiency and to determine true magnitudes of exergy losses that are proportional to the entropy generation. So, the universal exergy efficiency of assumed microtubes are calculated by Eq. (20) and presented in Figure 8. Regarding to Figure 8, it can be seen that exergy efficiency decreases as flow rate and coil diameter increase in each geometry.

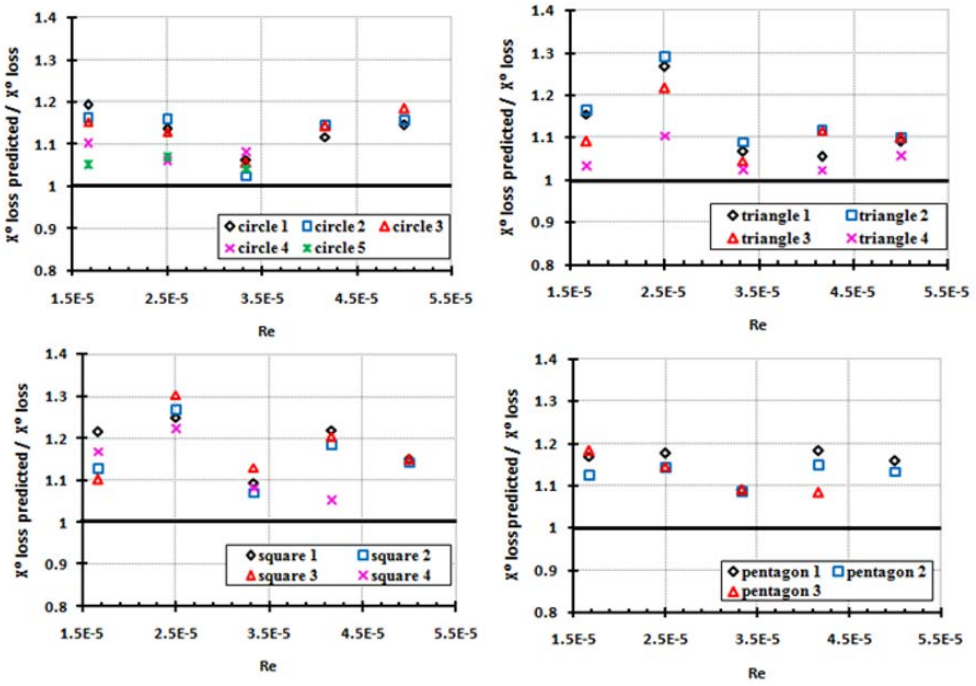

Figure 7. Dimensionless exergy losses versus Reynolds number in laminar flow range in different coil diameters of A) Circles, B) Triangles, C) Squares, and D) Pentagons

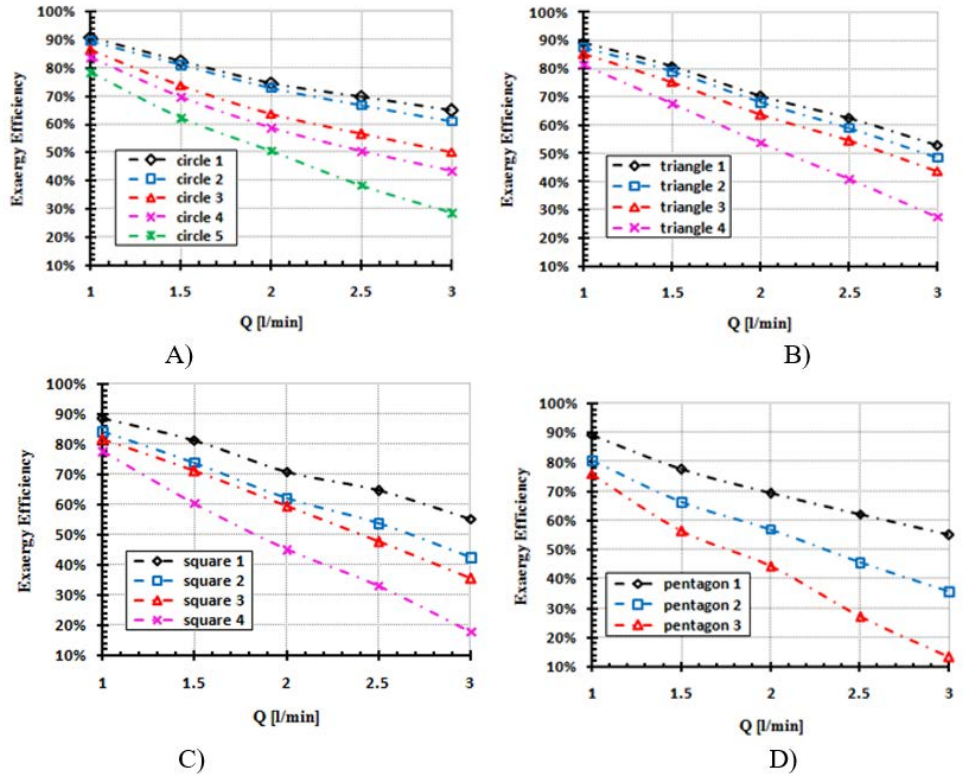

Figure 8. Exergy efficiencies versus flow rates in different coil diameters of A) Circles, B) Triangles, C) Squares, D) Pentagons

5 Conclusions

In a nutshell in this paper, an experimental investigation is executed to examine the entropy generation, exergy loss, and exergy efficiency of air flow through the adiabatic helical microtubes with unprecedented geometries. The

effects of air flow rate, coil diameter, and Dean number are inspected. The exergy loss is a measure to evaluate the thermodynamic efficiency of the process, in the other words, the lower exergy loss means the higher thermodynamic efficiency and the lower required energy, which can be achieved by debilitating irreversibility through friction. In the present study, exergy losses are investigated in helical microtubes with novel geometries under adiabatic conditions to discover the effects of viscous dissipation. Moreover, the entropy generation analysis is conducted to evaluate the inefficiency in the studied geometries. This study is expected to provide a comprehensive performance overview of the evaluated configurations. The conclusions of this inquiry can be recapitulated as:

• By analyzing experimental data, it was observed that entropy generation increases by increasing the flow rate in all geometries.

• In all studied geometries of helical microtubes, the entropy generation ascended as the coil diameters become larger in all geometries.

• By considering geometry, in constant flow rate and identical coil diameter, the highest entropy generation can be approximately observed in the triangles, squares, pentagons, and circles, respectively because of greater minor losses of pressure caused by bend angle in geometries.

• In a constant flow rate with increasing coil diameter, which is associated with the decrease in Dean number, it can be observed that the entropy generation is increased.

• The exergy efficiency decreases as flow rate and coil diameter increase in all geometries.

• The proportions of theoretical exergy losses to actual exergy losses have been computed for all geometries in order to probe the viscous heating effects. It is found that viscous heating effect should be accounted for air flow applications in the assumed microtubes. In other words, the viscous heating effect on entropy generation in the laminar flow regime can't be ignored.

• The results of comparing the measured and predicted values for exergy losses prove the experimental success of providing adiabatic conditions.

Data Availability

The data used to support the findings of this study are available from the corresponding author upon request.

Conflicts of Interest

The authors declare no conflict of interest.

References

[1] B. H. Salman, H. A. Mohammed, K. M. Munisamy, and A. S. Kherbeet, "Characteristics of heat transfer and fluid flow in microtube and microchannel using conventional fluids and nanofluids: A review," *Renew. Sustain. Energy Rev.*, vol. 28, pp. 848–880, 2013. https://doi.org/10.1016/j.rser.2013.08.012

[2] M. Moawed, "Experimental study of forced convection from helical coiled tubes with different parameters," *Energ. Convers. Manage*, vol. 52, no. 2, pp. 1150–1156, 2011. https://doi.org/10.1016/j.enconman.2010.09.009

[3] T. H. Ko, "Thermodynamic analysis of optimal mass flow rate for fully developed laminar forced convection in a helical coiled tube based on minimal entropy generation principle," *Energ. Convers. Manage*, vol. 47, no. 18-19, pp. 3094–3104, 2006. https://doi.org/10.1016/j.enconman.2006.03.006

[4] A. Bejan, "Entropy generation minimization: The new thermodynamics of finite-size devices and finite-time processes," *J. Appl. Phys.*, vol. 79, no. 3, pp. 1191–1218, 1996. https://doi.org/10.1063/1.362674

[5] A. A. Ozalp, "Entropy analysis of laminar-forced convection in a pipe with wall roughness," *Int. J. Exergy*, vol. 6, no. 2, pp. 249–275, 2009. https://doi.org/10.1504/IJEX.2009.024001

[6] A. A. Ozalp, "1st and 2nd law characteristics in a micropipe: integrated effects of surface roughness, heat flux and reynolds number," *Heat Transf. Eng.*, vol. 30, no. 12, pp. 973–987, 2009. https://doi.org/10.1080/01457630902837467

[7] H. S. Dizaji, S. Khalilarya, S. Jafarmadar, M. Hashemian, and M. Khezri, "A comprehensive second law analysis for tube-in-tube helically coiled heat exchangers," *Exp. Thermal Fluid Sci.*, vol. 76, pp. 118–125, 2016. https://doi.org/10.1016/j.expthermflusci.2016.03.012

[8] S. Pourhedayat, H. S. Dizaji, S. Jafarmadar, and S. Khalilarya, "An empirical correlation for exergy destruction of fluid flow through helical tubes," *Appl. Thermal Eng.*, vol. 140, pp. 679–685, 2018. https://doi.org/10.1016/j.applthermaleng.2018.05.065

[9] H. Moradi, A. Bagheri, M. Shafaee, and S. Khorasani, "Experimental investigation on the thermal and entropic behavior of a vertical helical tube with none-boiling upward air-water two-phase flow," *Appl. Thermal Eng.*, vol. 157, p. 113621, 2019. https://doi.org/10.1016/j.applthermaleng.2019.04.031

[10] T. H. Ko and K. Ting, "Entropy generation and thermodynamic optimization of fully developed laminar convection in a helical coil," *Int. Commun. Heat Mass Transfer*, vol. 32, no. 1-2, pp. 214–223, 2005. https://doi.org/10.1016/j.icheatmasstransfer.2004.04.039

[11] N. Parlak, M. Gür, V. Arı, H. Küçük, and T. Engin, "Second law analysis of water flow through smooth microtubes under adiabatic conditions," *Exp. Thermal Fluid Sci.*, vol. 35, no. 1, pp. 60–67, 2011. https://doi.org/10.1016/j.expthermflusci.2010.08.006

[12] N. Parlak, M. Gur, T. Engin, and H. Kucuk, "Exergy analysis of laminar fluid flow in stainless steel microtubes," *Int. J. Exergy*, vol. 9, no. 4, pp. 472–485, 2011. https://doi.org/10.1504/IJEX.2011.043918

[13] R. A. Rezaei, S. Jafarmadar, and S. Khorasani, "Presentation of frictional behavior of micro helical tubes with various geometries and related empirical correlation; an experimental study," *Int. J. Therm. Sci.*, vol. 140, pp. 377–387, 2019. https://doi.org/10.1016/j.ijthermalsci.2019.03.011

[14] R. J. Moffat, "Describing the uncertainties in experimental results," *Exp. Thermal and Fluid Science*, vol. 1, no. 1, pp. 3–17, 1988. https://doi.org/10.1016/0894-1777(88)90043-X

[15] I. Dincer and M. A. Rosen, *Exergy: Energy, environment and sustainable development*. Oxford, UK: Elsevier, 2012.

Nomenclature

S°_{gen}	Entropy generation,$\mathrm{W.K^{-1}}$
X°_{loss}	Exergy loss, W
h	Enthalpy, $\mathrm{kJ.kg^{-1}}$
m°	Mass flow rate, $\mathrm{kg.s^{-1}}$
ΔP	Pressure drop, KPa
Re	Reynolds number
D_c	Coil diameter, m
d	Tube diameter, m
D_e	Dean number
V	Velocity, $\mathrm{m.s^{-1}}$
T	Temperature, K
L	Tube length before coiling operation, m
f_c	Friction factor for helical microtubes
R	the specific ideal gas constant of the air

Greek symbols

$\boldsymbol{\rho}$	Density, $\mathrm{kg \cdot m^{-3}}$
ϑ	Kinematic viscosity

Subscripts

0	ambient
s	source
$outt$	outer
in	inlet
out	outlet